











RESEARCH

Open Access



# Boosting neuregulin 1 type-III expression hastens SMA motor axon maturation

Lingling Kong<sup>1†</sup>, Cera W. Hassinan<sup>1†</sup>, Florian Gerstner<sup>2</sup>, Jannik M. Buettner<sup>2</sup>, Jeffrey B. Petigrow<sup>1</sup>, David O. Valdivia<sup>1</sup>, Michelle H. Chan-Cortés<sup>1</sup>, Amy Mistri<sup>1</sup>, Annie Cao<sup>1</sup>, Scott Alan McGaugh<sup>1</sup>, Madeline Denton<sup>1</sup>, Stephen Brown<sup>1</sup>, Joshua Ross<sup>1</sup>, Markus H. Schwab<sup>3</sup>, Christian M. Simon<sup>2</sup> and Charlotte J. Sumner<sup>1,4\*</sup>

## Abstract

Intercellular communication between axons and Schwann cells is critical for attaining the complex morphological steps necessary for axon maturation. In the early onset motor neuron disease spinal muscular atrophy (SMA), many motor axons are not ensheathed by Schwann cells nor grow sufficiently in radial diameter to become myelinated. These developmentally arrested motor axons are dysfunctional and vulnerable to rapid degeneration, limiting efficacy of current SMA therapeutics. We hypothesized that accelerating SMA motor axon maturation would improve their function and reduce disease features. A principle regulator of peripheral axon development is neuregulin 1 type III (NRG1-III). Expressed on axon surfaces, it interacts with Schwann cell receptors to mediate axon ensheathment and myelination. We examined NRG1 mRNA and protein expression levels in human and mouse SMA tissues and observed reduced expression in SMA spinal cord and in ventral, but not dorsal root axons. To determine the impact of neuronal NRG1-III overexpression on SMA motor axon development, we bred NRG1-III overexpressing mice to SMA $\Delta$ 7 mice. Neonatally, elevated NRG1-III expression increased SMA ventral root size as well as axon segregation, diameter, and myelination resulting in improved motor axon conduction velocities. NRG1-III was not able to prevent distal axonal degeneration nor improve axon electrophysiology, motor behavior, or survival of older mice. Together these findings demonstrate that early SMA motor axon developmental impairments can be ameliorated by a molecular strategy independent of SMN replacement providing hope for future SMA combinatorial therapeutic approaches.

**Keywords** Spinal muscular atrophy (SMA), Motor axon, Neuregulin 1 type III (NRG1-III), Conduction velocity, Neuromuscular junction (NMJ)

## Introduction

The motor neuron (MN) disease spinal muscular atrophy (SMA) is caused by recessive mutations of the survival motor neuron 1 (*SMN1*) gene, retention of variable copies of an alternatively spliced, paralogous gene *SMN2*, and deficient expression of the SMN protein [25, 26, 28]. Severely affected patients who have only two copies of *SMN2* experience severe muscle weakness within weeks or months of birth. Three disease modifying treatments—the antisense oligonucleotide nusinersen, the gene replacement therapy onasemnogene abeparvovec, and small molecule risdiplam—increase SMN levels,

<sup>†</sup>L. Kong and C. W. Hassinan are co-first authors

\*Correspondence:

Charlotte J. Sumner  
csumner1@jhmi.edu

Full list of author information is available at the end of the article



but therapeutic efficacy is limited in part by early neurodegeneration [31]. This is evidenced by measurement of neurofilament (NF) levels released into serum or cerebrospinal fluid (CSF) from axons during degeneration. Serum and CSF NFs are most elevated in severe SMA patients neonatally, even prior to detectable muscle weakness, and thereafter decline [8, 9].

In an effort to understand the cellular basis of this early degeneration, we recently characterized MNs and their axons in severe SMA patient human tissues and in a severe SMA mouse model (SMA $\Delta$ 7 mice) [22]. We observed that many SMA motor axons and their surrounding Schwann cells are slowed in their development beginning in utero. In order to acquire a large myelinated axon phenotype capable of rapid conduction velocities, individual motor axons must progress through a series of morphological stages becoming individually ensheathed by Schwann cell cytoplasm, segregated 1:1 with Schwann cells after Schwann cell proliferation, and myelinated proportionate to radial diameter [13, 49]. Instead, many SMA motor axons are stalled in clusters of directly abutting, small axons less than 1  $\mu$ m in diameter associated with a reduced number of Schwann cells. Although some SMA motor axons mature sufficiently to become myelinated, they are reduced in diameter and have slowed conduction velocities. These developmental impairments precede neurodegeneration with the most developmentally lagging axons vulnerable to rapid degeneration neonatally [22]. Suboptimal efficacy of current therapeutics in some SMA patients likely results from failure to reverse developmental abnormalities as well as prevent neurodegeneration. Indeed, in severe SMA mice, prenatal rather than postnatal initiation of a risdiplam analogue was required to improve the maturation and maintenance of the most developmentally impaired SMA motor axons [22]. Strategies to accelerate SMA motor axon maturation *postnatally* have the potential to prevent their early degeneration and improve their function. Recent electrophysiological studies suggest that partial improvements in axonal maturation in SMA patients treated with nusinersen are associated with gains in motor function [20, 21].

The molecular mechanisms underlying impaired motor axon maturation in SMA are unknown. The completion of a complex series of morphological steps for axon radial maturation requires bidirectional signaling between axons and Schwann cells [12, 46]. Neuregulin 1 (NRG1) is a member of an epidermal growth factor (EGF)-like family of growth factors that plays essential roles in nervous system development and nerve repair [3]. The human *NRG1* gene encodes 6 principal NRG1 isoforms via alternative splicing and differential promoter usage [7]. NRG1-III is the major isoform produced by MNs in the

developing spinal cord [23, 32]. It is a membrane tethered growth factor where it interacts with ErbB2/3 receptors on Schwann cells. It is essential for Schwann cell proliferation, motility, survival, and peripheral axon ensheathment and myelination with the amount of NRG1-III determining the ensheathment fate and myelin thickness of an axon [33, 39, 47]. NRG1 also helps maintain the functional integrity and survival of peripheral nerve axons and therefore NRG1/ErbB signaling has also been considered a potential therapeutic target in neurodevelopmental and neurodegenerative diseases [40, 44].

Here, after observing that NRG1 expression was reduced in SMA human and mouse tissues, we assessed whether boosting NRG1-III expression in SMA mice could improve motor axon maturation. Importantly, NRG1-III overexpression increased SMA motor axon ensheathment and myelination in neonatal SMA mice resulting in increased conduction speed. Although NRG1-III did not prevent distal axonal degeneration nor provide long term benefit to SMA mice, this study is an important proof of principle that SMA axonal developmental phenotypes can be ameliorated with therapeutic strategies independent of SMN induction opening the possibility to future combination therapeutic strategies.

## Material and methods

### Human samples

De-identified human cervical spinal cord (CSC), ventral root (VR), and dorsal root (DR) tissues (Table 1) were collected at expedited autopsies following parental- or patient-informed consent in strict observance of legal and institutional ethical regulations as previously described [22, 42].

### Mouse lines and assessments

Experiments were performed in accordance with the National Institutes of Health Guide for Care and Use of Laboratory Animals and approved by Institutional Animal Care and Use Committees (IACUCs) at Johns Hopkins University School of Medicine and Leipzig University. SMA $\Delta$ 7 (JAX#00,525) mice were bred to hemizygous Thy1.2-HA-NRG1-III “HANI” mice originated from Max Planck Institute of Experimental Medicine in Göttingen, Germany. SMA $\Delta$ 7 mice were genotyped as previously described [41] and the *NRG1 Type III* transgene was genotyped using the following primers: forward primer 5'-GGCTTCTCTGAGTGGCAAAGGACC -3', reverse primer 5'-GTCCACAAATACCCACTTTAGGCCAGC -3'. Investigators were blinded to mouse genotypes during phenotypic assessments, which included

**Table 1** Human tissues

Case ID	Age (months)	PMI (hours)	SMN1 copy #	SMN2 copy #	Tissue	Cause of death
CNTL 12-02	0.03	26	2	2	L3 VR, L5 DR,	Unknown
CNTL 90-08	1.3	8	2	2	CSC	Arthrogryposis
CNTL 02-02	3	15	2	2	CSC	Nemaline myopathy
CNTL 08-01	4	14.5	2	2	L4 VR, CSC	Unknown
CNTL 95-03	6	8	N/A	N/A	CSC	Megacystis microcolon
CNTL 17-01	9	14	N/A	N/A	L1 VR, L1 DR	Trisomy 21, viral pneumonia
CNTL 12-05	19	19	2	1	L3 VR, L3 DR	Unknown
SMA 11-01	1.8	7	0	2	L2 VR, L2 DR, CSC	Type 1 SMA
SMA 12-01	2.5	7	0	2	L3 VR, L2 DR, CSC	Type 1 SMA
SMA 09-02	4	4	0	2	CSC	Type 1 SMA
SMA 92-01	5.5	14	0	2	CSC	Type 1 SMA
SMA 10-14	7	25	0	2	L1 VR, L3 DR	Type 1 SMA
SMA 14-05	8	6	0	2	CSC	Type I SMA
SMA 94-06	12.8	10	0	2	CSC	Type 1 SMA
SMA 14-04	72	24	0	2	L4 VR	Type 1 SMA

PMI = post-mortem interval, CNTL = non-SMA control subject, SMA = SMA subject, CSC = cervical spinal cord, DR = dorsal root, L = lumbar, VR = ventral root, N/A = not available

daily body weights, righting time and survival [22]. Post-natal day 1 (P1) was defined as the day of birth.

#### RNA isolation and RT-qPCR analysis

RNA was isolated using TRIzol reagent (Thermo Fisher Scientific) and RT-qPCR was performed as previously described [22]. Custom Primers used to amplify human *NRG1 Type I* were: forward 5'-GCCAATATCACCATC GTGGAA-3', reverse 5'-CCTTCAGTTGAGGCTGGC ATA-3', and probe 5'-FAM-CAAACGAGATCATCA CTG-MGB-3'. Primers used to amplify human *NRG1 Type III* were: forward 5'-CAGCCACAAACAACAGAA ACTAATC-3', reverse 5'-CCCAGTGGTGGATGTAGA TGTAGA-3', and probe 5'-FAMCCAAACTGCTCC TAAAC-MGB-3' [16]. Primers used to amplify mouse *NRG1 Type I* were Mm00626552\_m1 (ThermoFisher) and *NRG1 Type III* Mm01212129\_m1 (ThermoFisher).

#### Western blot analysis

Western blots were completed as previously described [29]. Proteins were separated by size and transferred onto a 0.2 µm polyvinylidene difluoride (PVDF) membrane (ThermoFisher). Antibodies used were rat anti-HA antibody (Millipore Sigma), mouse anti-SMN antibody (BD Transduction Laboratories) and mouse anti-GAPDH (ThermoFisher) antibody.

#### Immunohistochemistry

Mice were transcardially perfused with 4% paraformaldehyde (PFA) and post-fixed in PFA. Spinal cords were embedded in warm 5% Agar and serial transverse

Sects. (75 µm) were cut on a vibratome. Primary antibodies included anti-ChAT (goat, AB144P, Merck) 1:250 and NRG1 C-terminal antibody, anti-NRG1 (rabbit, SC-348, Santa Cruz) 1:300. Secondary antibodies included the appropriate species-specific antiserum coupled to Alexa488, Cy3 or Cy5 (Jackson labs). Sections were imaged using a SP8 Leica confocal microscope [5] and NRG1 spots in ChAT + MNs from at least 3 animals per genotype were counted using LASX software from z-stack images (complete MN somata at 4 µm intervals in the z axis). Only whole ChAT + MNs that contained the nucleus were included for quantification.

VRs and DRs were sectioned (20 µm thick) on a cryostat (Leica) and stained with primary antibodies against Tuj1 (Chicken IgY, 1:1000), NFH (MsIgG1, 1:1000, Biolegend) and anti-NRG1 (rabbit, 1:400, Santa Cruz). Secondary antibodies included Alexa Fluor (AF) 633 Goat-anti-rabbit (1:500, Invitrogen), AF546 Goat-anti-chicken, (1:1000, Invitrogen), and AF488 Goat-anti-Ms IgG1, 1:200 (Jackson Immunology). Sections were imaged using a Zeiss Confocal Laser Microscope. Neuromuscular junctions (NMJs) were examined in teased myofibers of quadratus lumborum (QL) muscles [22] and labeled using monoclonal mouse anti-SMI 312 (1:1000; Biolegend) and polyclonal rabbit anti-synaptophysin (1:500; Invitrogen) antibodies, followed by AF488 goat anti-mouse IgG1 (1:200; Jackson Immunoresearch Laboratories), AF 633-conjugated goat anti-rabbit secondary antibody (1:1000; Invitrogen), and α-Bungarotoxin AF-555 (1:500; Invitrogen).

### Light and electron microscopy

VRs and DRs were post-fixed using 2% osmium tetroxide and embedded in propylene oxide and EMBED 812 plastic (Electron Microscopy Sciences). Thick Sects. (1  $\mu$ m) were cut, stained with toluidine blue, and imaged using a Zeiss Axiovision microscope. Area and number of myelinated axons were counted using ZenLite software [22]. For electron microscopy (EM), thin sections were cut at 60–90 nm, placed on bar-less formvar grids, and viewed using a Libra 120 (Zeiss) transmission EM. Consecutive overlapping images were taken at 8000 $\times$  or 16,000 $\times$  and reconstructed using Adobe Photoshop. The number of axons, axon diameters, and G-ratios were quantified in reconstructed VR images using Zen lite software.

### Serum NF quantification

Cardiac puncture was performed using a 31-gauge syringe for blood collection into a Protein LoBind microcentrifuge tube (500  $\mu$ l). Serum was isolated and NF-L concentrations were determined using the single molecule array (Simoa) Quanterix platform with NF-Light<sup>®</sup> (SR-X) kit (Quanterix 103,400) and SR-X instrument [22].

### Electrophysiology

The function of motor axons and NMJs innervating the QL muscle were assessed as previously described [6, 22]. Animals were decapitated, the torso transferred into a dissecting chamber with cold ( $\sim$ 12  $^{\circ}$ C) oxygenated (95%O<sub>2</sub>/5%CO<sub>2</sub>) artificial cerebrospinal fluid (aCSF) containing 128.35 mM NaCl, 4 mM KCl, 0.58 mM NaH<sub>2</sub>PO<sub>4</sub>, H<sub>2</sub>O, 21 mM NaHCO<sub>3</sub>, 30 mM D-Glucose, 1.5 mM CaCl<sub>2</sub>·H<sub>2</sub>O, and 1 mM MgSO<sub>4</sub>·7H<sub>2</sub>O. After a laminectomy, the spinal cord was removed, leaving the lumbar level 1 (L1) VR intact in continuity with the QL muscle. MN axons in the L1 VR supplying the QL muscle were stimulated, and the compound muscle action potential (CMAP) was recorded from the muscle using a concentric bipolar electrode. L1 MN axons were stimulated with five stimuli at 1 Hz for peak-to-peak measurements of the maximum CMAP amplitude from five averages.

The extracellular recorded potentials were recorded (DC – 3 kHz, Cyberamp, Molecular Devices) in response to a brief (0.2 ms) stimulation (A365, current stimulus isolator, WPI, Sarasota, FL) of the L1 VR. Recordings were fed to an A/D interface HEKA EPC10/2 amplifier (HEKA Elektronik, Lambrecht/Pfalz, Germany) and acquired with HEKA Patchmaster (HEKA Electronics) amplifier at a sampling rate of 20 kHz. Data were analyzed offline using HEKA Patchmaster (HEKA Electronics). The latency was determined by measuring the time between the beginning of the stimulus artifact and the onset of the CMAP response. The conduction velocity was calculated by the time of the latency minus the time of synaptic transmission, divided by the distance of the stimulating and recording electrode.

### Statistical analysis

Data were expressed as means  $\pm$  SEM with at least three independent samples per group. Differences between two groups were analyzed by a two-tailed unpaired Welch's t test or Mann–Whitney for nonparametric analysis, where appropriate, using GraphPad Prism 9. Differences among three or more groups were analyzed with one-way analysis of variance (ANOVA) using Tukey's post hoc correction. Survival curves were compared using log-rank test.

### Results

#### NRG1 expression is reduced in SMA

We examined mRNA expression levels of two isoforms of NRG1: NRG1-III, which is abundant in developing MNs and axons [32], and NRG1-I, which is expressed in Schwann cells during remyelination of peripheral nerves [45] (Fig. 1a). *NRG1-III*, but not *NRG1-I*, was reduced in postnatal day 1 (P1) SMA $\Delta$ 7 compared to wild type (WT) mouse spinal cords (Fig. 1b,c) as well as in human type I SMA compared to age-matched control spinal cords (Table 1, Fig. 1d,e). As NRG1 is enriched at the post-synaptic terminals of C-bouton synapses [15], we examined NRG1 expression on MNs in P2 and P12 lumbar level 1 (L1) and L5 mouse spinal cords using an

(See figure on next page.)

**Fig. 1** NRG1 expression is reduced in severe SMA mice and patients **A** Schematic of NRG1 protein isoforms, Type I and Type III. **B** Relative *NRG1-I* and **C** *NRG1-III* mRNA expression levels in spinal cords of WT and SMA mice at P1 (n = 3 each). **D** Relative *NRG1-I* and **E** *NRG1-III* mRNA expression levels in spinal cords of controls and SMA Type 1 cases. **F** Representative L1 MNs stained with ChAT (blue) and NRG1 (white) in WT and SMA mice at P12 (scale bar: 50  $\mu$ m). Quantification of NRG1 punctae on **G** L1 MNs, **H** L5 lateral motor column (LMC) MNs, and **I** L5 medial motor column (MMC) MNs from P2 WT and SMA mice (n = 3 each). **J** Representative LMC and MMC L5 MNs stained with ChAT (blue) and NRG1 (white) in WT and SMA mice at P12 (bottom scale bar: 100  $\mu$ m and top scale bar: 20  $\mu$ m.) Quantification of NRG1 punctae on **K** L1 MNs, **L** L5 LMC MNs, and **M** L5 MMC MNs in P12 WT and SMA mice (n = 3 each). **N** Representative confocal images of L1 VRs stained with NRG1 (red), Tuj1 (green), NFH (blue) in WT and SMA mice at P2 (scale bars: 10  $\mu$ m and magnified scale bar: 1  $\mu$ m). **O** Percentage of Tuj1 + overlap with NRG1 + over total Tuj1 + punctae of WT and SMA mice at P2 (n = 3 each) in L1 VRs and **P** DRs. **Q** Representative confocal images of human VRs stained with NRG1 (red), Tuj1 (green), PO (blue) from CNTL 12-02 and SMA 11-01 (scale bar: 20  $\mu$ m and magnified scale bar: 2.5  $\mu$ m). **R** Percentage of Tuj1 + overlap with NRG1 + over total Tuj1 + punctae in VRs of controls and SMA Type 1 cases and **S** in DRs of controls and SMA Type 1 cases. Data represents means and SEM. Statistical analysis was performed using unpaired t test. Significance: \* $p$   $\leq$  .05, \*\* $p$  < 0.01

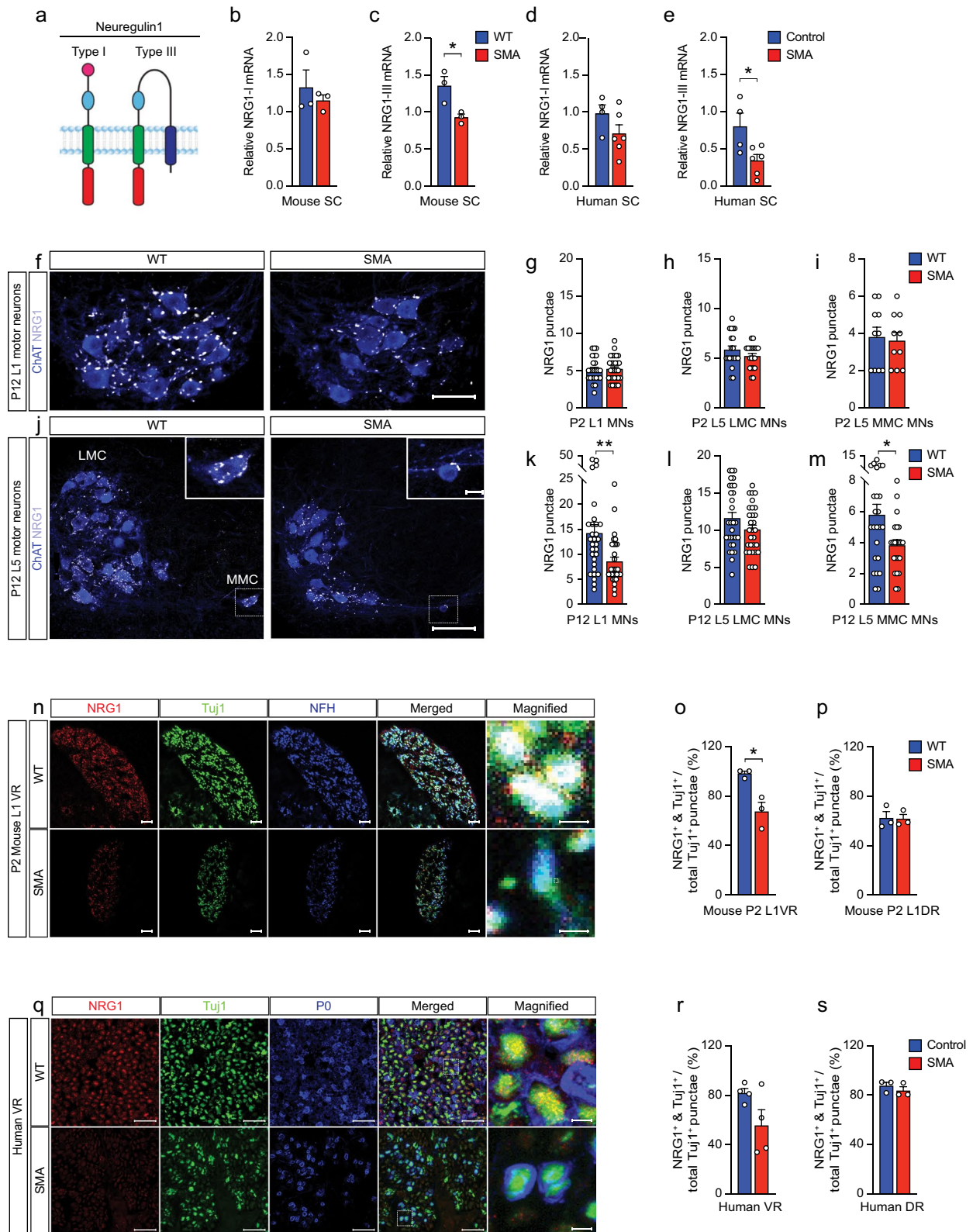


**Fig. 1** (See legend on previous page.)

antibody that recognizes all NRG1 isoforms. Although the number of NRG1 + punctae on L1 and L5 MNs was unchanged at P2 (Fig. 1g–i), they were reduced on P12 SMA L1 MNs and L5 medial motor column (MMC) MNs (Fig. 1f, j–m). We next examined NRG1 expression in L1 ventral roots (VRs) (containing motor axons) and dorsal roots (DRs) (containing sensory axons) [22]. In contrast to the late loss of NRG1 on MN somata, we observed a decrease in the percentage of Tuj1 positive punctae expressing NRG1 in SMA mouse VRs, but not DRs as early as P2 (Fig. 1n–p). The percentage of axons expressing Tuj1, NF-H, and NRG1 were also decreased in VRs of SMA compared to WT mice at P2 (WT =  $64.3 \pm 6.7\%$  vs. SMA =  $30.2 \pm 7.6\%$ ,  $p < 0.05$ ). The percentage of Tuj1<sup>+</sup> punctae expressing NRG1 was variable in human SMA VRs and when taken together did not show a significant decrease relative to controls ( $p = 0.097$ ) (Fig. 1q, r). However, the case with the highest value (SMA14-04) was substantially older at 72 months compared to the other 3 SMA cases, which were all  $\leq 7$  months old (Table 1). With this older case removed, there was a significant decrease ( $p = 0.007$ ) in the percentage in NRG1 + Tuj1 punctae in SMA VRs compared to controls. No decrease was observed in DRs (Fig. 1p, s). Taken together, these data indicated that NRG1 levels are reduced in SMA MN somata and axons of SMA mice and patients.

### Boosting NRG1-III expression hastens SMA motor axon development

To test whether increased NRG1-III expression would mitigate deficits of axon maturation in SMA mice, we bred SMA $\Delta 7$  mice to mice overexpressing N-terminally HA-tagged full-length *NRG1-III* cDNA under control of the neuronal Thy1.2 promoter (Thy1.2-HA-NRG1-III mice) [48] generating mice of the following genotypes: WT (*hSMN2<sup>+/+</sup>/SMA $\Delta 7^{+/+}$ /mSmn<sup>+/+</sup>*), WT NRG1-III + (*hSMN2<sup>+/+</sup>/SMA $\Delta 7^{+/+}$ /mSmn<sup>+/+</sup>/HA-NRG1-III*), SMA (*hSMN2<sup>+/+</sup>/SMA $\Delta 7^{+/+}$ /mSmn<sup>-/-</sup>*), and SMA-NRG1-III + (*hSMN2<sup>+/+</sup>/SMA $\Delta 7^{+/+}$ /mSmn<sup>-/-</sup>/HA-NRG1-III*) (Fig. 2a). Western blots from spinal cord lysates isolated from P10 mice demonstrated expression of the HA-NRG1-III protein in both WT NRG1-III + and SMA NRG1-III + mice, but not WT or SMA mice not harboring the *NRG1-III* transgene (Fig. 2b). The expression of NRG1-III did not alter the expression of SMN protein in WT or SMA mouse spinal cords (Additional file 1: Fig. S1).

We examined VRs at the L1 level, where we have previously shown that motor axons are particularly vulnerable to developmental defects [22] (Fig. 2c). SMA VRs were reduced in their cross sectional area and had fewer myelinated axons and Schwann cell nuclei compared to WT VRs (Fig. 2c–f). In WT mice, NRG1-III overexpression

increased myelinated axon number by 106%, but only showed a trend ( $p = 0.05$ ) to increased VR area and did not show a change in Schwann cell number (Fig. 2d–f). In contrast, boosting NRG1-III expression in SMA mice increased VR cross sectional area by 177%, the number of myelinated axons by 272%, and the number of Schwann cells by 89%, restoring each of these parameters to levels observed in WT mice not overexpressing NRG1-III (Fig. 2d–f).

At the electron microscopy (EM) level, boosting NRG1-III expression did not change the total number of axons in either WT or SMA mice (Fig. 3a, b). Motor axons were further classified based on developmental stage into abutting, ensheathed, segregated and myelinated types as defined previously [22]. In WT mice overexpressing NRG1-III, a decrease in the number of abutting axons was not accompanied by significant changes in other axon types (Fig. 3c). In contrast in SMA mice, a 437% increase in myelinated axon number and a 98% increase in segregated axon number indicated that NRG1-III not only reinstated myelination of axons, but also partially restored the sorting/segregation of axons by Schwann cells into the one-to-one relationships required for myelination (Fig. 3d).

To further characterize the myelinated motor axons, we determined their diameter and myelin thickness. In WT mice, NRG1-III overexpression did not increase the diameter of myelinated motor axons (mean WT =  $1.7 \mu\text{m}$  vs. WT NRG1-III + =  $1.8 \mu\text{m}$ ,  $p = 0.89$ ) (Fig. 3e, g), but did reduce the median G-ratio from 0.89 to 0.78 ( $p = 0.002$ ) indicating thicker myelin sheaths. In SMA mice, NRG1-III overexpression restored median axon diameter (SMA =  $1.5 \mu\text{m}$  vs. SMA NRG1-III + =  $2.0 \mu\text{m}$ ,  $p = 0.002$ ) as well as the percentage of myelinated axons with a diameter between 1.5 and  $3 \mu\text{m}$  to WT levels (Fig. 3f, g). Additionally, while median G-ratio was unchanged, boosting NRG1-III expression increased the percentage of SMA myelinated axons with lower G-ratio = 0.6–0.8 and decreased those with a higher G-ratio = 0.8–1.0 (Fig. 3f, h). These data indicate that in SMA but not WT mice, boosting NRG1-III expression accelerated multiple motor axon developmental steps including radial growth, Schwann cell segregation and myelination.

### NRG1-III overexpression improves neonatal motor axon conduction velocity, but does not prevent axon degeneration

To assess whether the improvements in early SMA motor axon development were associated with alterations in function, we performed electrophysiology using ex vivo nerve muscle preparations (Fig. 4a, b). Consistent with prior observations, the conduction velocity of SMA motor axons was reduced compared to WT mice

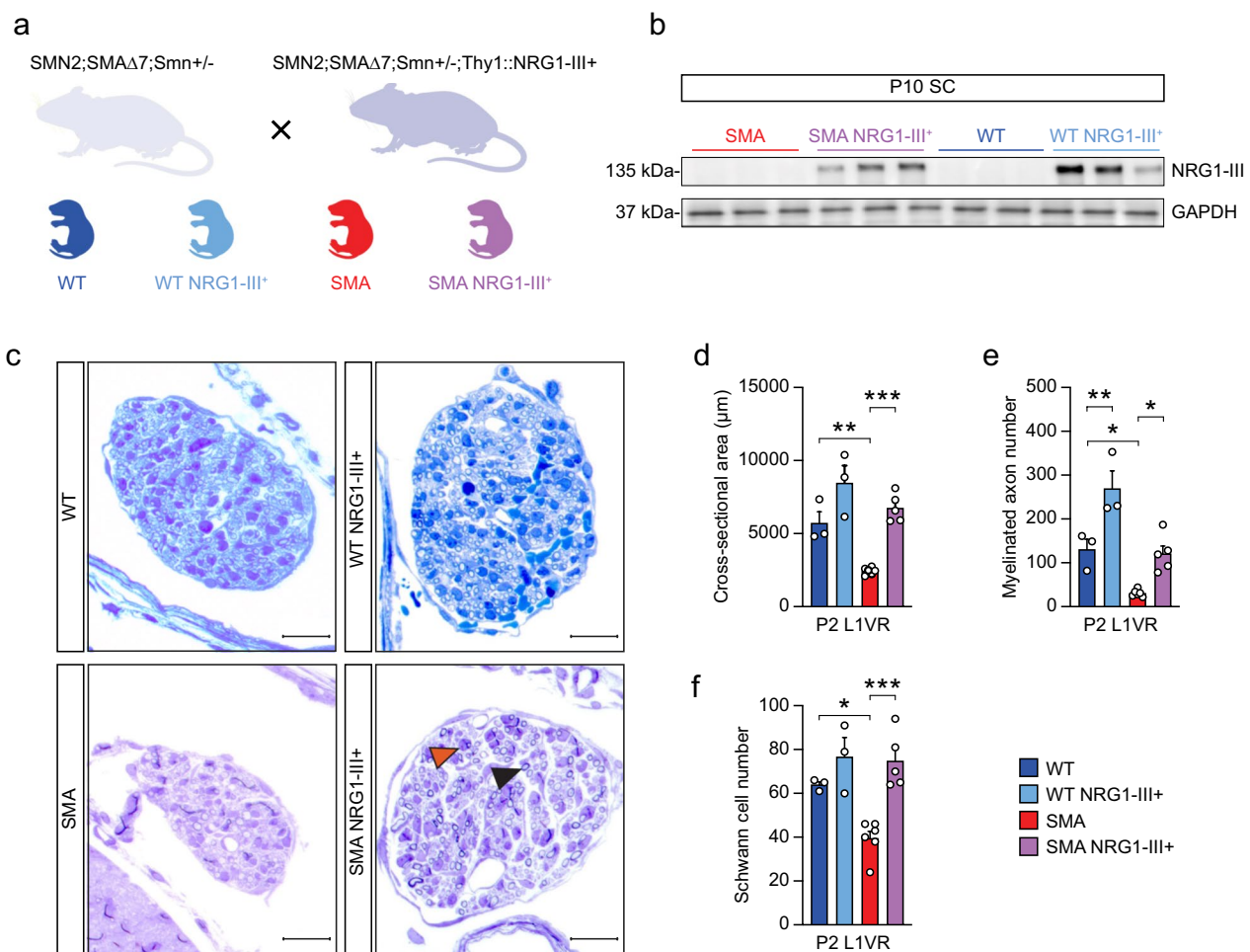


**Fig. 2** Boosting NRG1-III expression in SMA mice increases VR myelinated axon number **A** Schematic of mouse breeding to generate genotypes: WT, WT NRG1-III<sup>+</sup>, SMA, and SMA NRG1-III<sup>+</sup>. **B** Western blot of NRG1-III protein expression in spinal cord protein lysates collected from WT, WT NRG1-III<sup>+</sup>, SMA, and SMA NRG1-III<sup>+</sup> mice at P10 (n = 3 each). **C** Representative toluidine blue-stained cross sections of L1 VRs in WT, WT NRG1-III<sup>+</sup>, SMA, and SMA NRG1-III<sup>+</sup> of mice at P2 (scale bar: 20  $\mu\text{m}$ ). The black arrow indicates a myelinated axon and the orange arrow indicates a Schwann cell nucleus. **D** Cross-sectional area, **E** myelinated axon number and **F** Schwann cell number in L1 VRs from WT (n = 3), WT NRG1-III<sup>+</sup> (n = 3), SMA (n = 6), and SMA NRG1-III<sup>+</sup> (n = 5) mice at P2. Data represent means and SEM. Statistical analysis was performed **D–F**, using one-way ANOVA. Significance of WT compared to SMA NRG1-III<sup>+</sup> and WT NRG1-III<sup>+</sup> compared to SMA not included. Significance: \* $p \leq .05$ , \*\* $p < 0.01$ , \*\*\* $p < 0.001$

(Fig. 4c). In both WT and SMA mice, NRG1-III overexpression increased conduction velocity with SMA mice reaching similar levels to WT mice (Fig. 4c). Despite this improvement, which likely relates to the increased number, diameter and myelin thickness of myelinated SMA motor axons, the compound muscle action potential (CMAP) amplitudes, which represent the summated voltage responses from the individual muscle fiber action potentials generated by the most rapidly conducting axons, was not increased by NRG1-III overexpression in SMA mice (Fig. 4d).

Unchanged CMAP amplitudes in SMA NRG1-III overexpressing mice suggest an ongoing inability of

motor axons to stimulate a muscle action potential. We thus examined the innervation status of neuromuscular junctions (NMJs) in the quadratus lumborum (QL) muscle using immunohistochemistry. As expected, there was an increase in the number of denervated NMJs in the QL of SMA compared to WT mice, but NRG1-III overexpression did not alter these denervation percentages (Fig. 4e,f) nor did it suppress levels of serum NF-L in SMA mice (Fig. 4g). Together these data indicate that NRG1-III overexpression does not suppress degeneration of the distal motor axon in SMA mice.

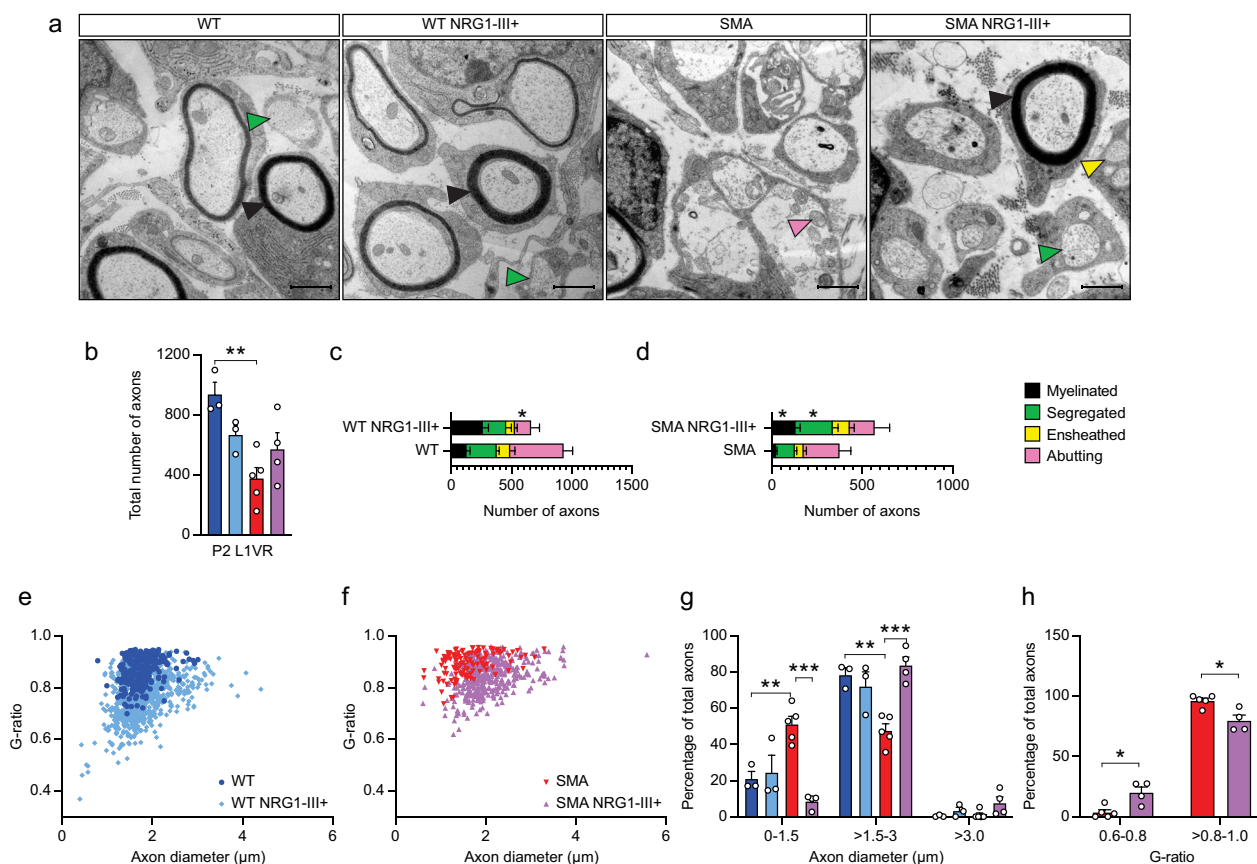


**Fig. 3** NRG1-III overexpression accelerates several aspects of motor axon development in SMA mice **A** Representative EM images of L1 VRs in WT, WT NRG1-III +, SMA, and SMA NRG1-III + mice at P2 (scale bar: 1 μm). The black, green, yellow, and pink arrows indicate myelinated, segregated, ensheathed and abutting axons, respectively. **B** Quantification of total number of axons in L1 VRs of WT (n = 3), WT NRG1-III + (n = 3), SMA (n = 5), and SMA NRG1-III + (n = 4) mice at P2; separated by axon category for WT and WT NRG1-III + **C** and SMA and SMA NRG1-III + **D** mice. **(E and F)** Axon diameters and G-ratios of L1 VRs in WT and WT NRG1-III + **E** and SMA and SMA NRG1-III + **F** mice. **G** Percentage of axons by axon diameter for each genotype. **H** Percentage of axons by different G-ratio categories for SMA and SMA NRG1-III + mice. Data represents means and SEM. Statistical analysis was performed **(B)** and **(H)**, using one-way ANOVA; in **(C)**, **(D)** and **(G)** using unpaired t test. Significance of WT compared to SMA NRG1-III + and WT NRG1-III + compared to SMA not included. Significance: \* $p \leq .05$ , \*\* $p < 0.01$ , \*\*\* $p < 0.001$

### NRG1-III does not provide sustained benefit to SMA motor axons

In order to assess the longer-term consequences of NRG1-III overexpression on WT and SMA mice, we characterized mouse survival, weight, and time to right (Additional file 2: Fig. S2). Boosting NRG1-III expression did not ameliorate deficits in SMA mice; rather survival was reduced by NRG1-III overexpression ( $p = 0.006$ ). We also examined the electrophysiology and structure of motor axons at P12 compared to P2 (Figs. 4b–d and 5a–c). CVs increased by 497% ( $p = 0.001$ ) and 257% ( $p < 0.001$ ) between P2 and P12 in WT and WT NRG1-III + mice, respectively (Figs. 4c and 5b). This increase of CV was associated with decreases in G-ratios [25% in WT ( $p < 0.001$ ) and 20% in WT NRG1-III + ( $p = 0.029$ )] and a 32% increase in myelinated axon diameter in WT mice ( $p < 0.001$ ) (Figs. 3e and 5h). Between P2 and P12, CMAP amplitudes increased

by 239% ( $p = 0.009$ ) in WT mice and 376% ( $p = 0.017$ ) in WT NRG1-III + mice (Figs. 4d and 5c) corresponding with a 193% increase in myelinated axon number in WT mice ( $p < 0.001$ ) (Figs. 2e and 5e). In contrast, SMA and SMA NRG1-III + mice showed no increases in CMAP amplitudes between P2 and P12 likely due to ongoing axon degeneration mitigating any developmental gains. While at P2, NRG1-III was able to restore myelinated axon number, myelinated axon diameter, and conduction velocity in SMA mice to WT levels, further developmental gains in axonal diameter and conduction velocity did not occur in SMA NRG1-III + mice between P2 and P14 (Fig. 5d–f). NRG1-III overexpression did increase the percentage of SMA axons with thick myelin sheaths (G-ratio  $> 0.4–0.6$ ), but in the absence of an increase in axon diameter, this was not sufficient to increase CV (Fig. 5g,i,j).



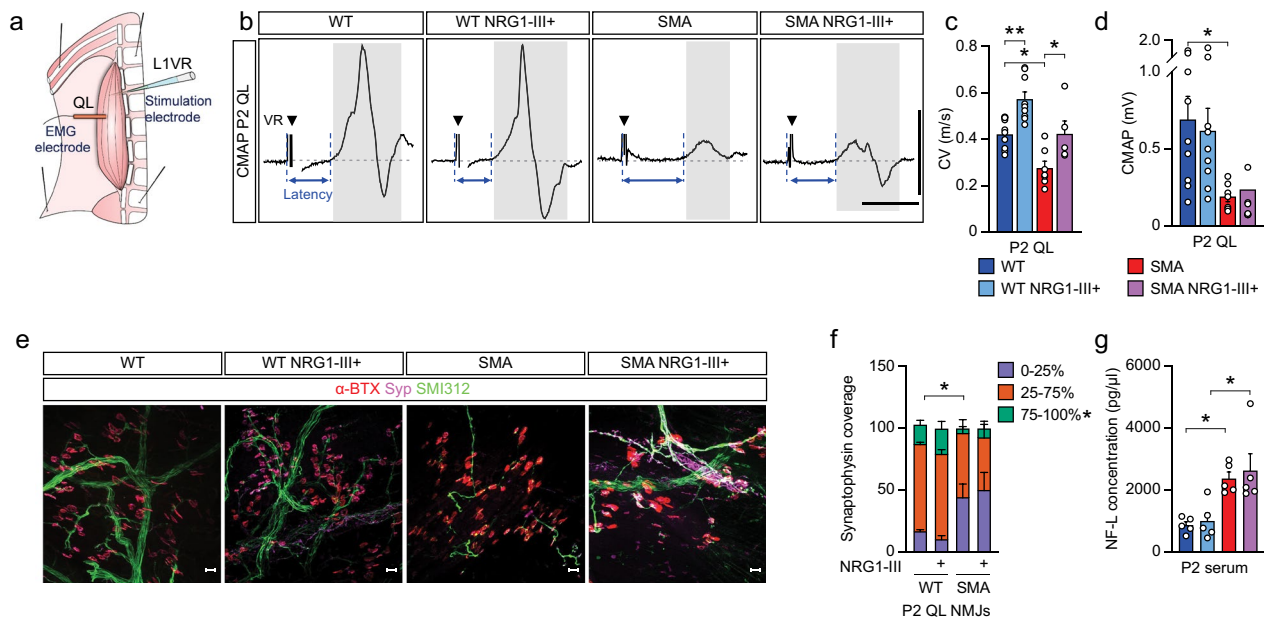


**Fig. 4** NRG1-III improves neonatal SMA motor axon conduction speed but does not prevent degeneration **A** A schematic of the ex vivo nerve muscle preparations for stimulating L1 VR and recording from the quadratus lumborum (QL) muscle. **B** Representative traces from the QL muscle in WT, WT NRG1-III+, SMA, and SMA NRG1-III+ mice at P2. **C** Conduction velocity and **D** CMAP amplitude from the QL muscle of WT ( $n = 9$ ), WT NRG1-III+ ( $n = 9$ ), SMA ( $n = 7$ ), and SMA NRG1-III+ ( $n = 5$ ) mice at P2. **E** Representative confocal images of P2 QL muscle NMJs stained with  $\alpha$ -bungarotoxin ( $\alpha$ -BTX, red), synaptophysin (Syp, purple), and SMI312 (green) (scale bar: 20  $\mu$ m). **F** NMJ innervation in the L1 QL muscle of WT, WT NRG1-III+, SMA, and SMA NRG1-III+ ( $n = 3$  each) mice at P2. **G** Serum NF-L concentration of WT, WT NRG1-III+, SMA, and SMA NRG1-III+ ( $n = 5$  each) mice at P2. Data represents means and SEM. Statistical analysis was performed in (**C**, **D**) and (**G**) using one-way ANOVA; and in (**F**) using unpaired t test. Significance of WT compared to SMA NRG1-III+ and WT NRG1-III+ compared to SMA not included. Significance: \* $p \leq 0.05$ , \*\* $p < 0.01$

## Discussion

In the most common severe SMA patient group, degeneration of the most immature motor axons is most evident neonatally and may even begin in utero [22]. The molecular mechanisms downstream of SMN deficiency that underlie slowed axon development and degeneration are unknown. Here, we explored the role of NRG1-III, levels of which are a principal determinant of peripheral axon Schwann cell ensheathment and myelination. We demonstrated that NRG1 expression is reduced in both severe human and mouse SMA spinal cords and VRs. Supporting the conclusion that NRG1-III directly contributes to retarded axon development in SMA, boosting NRG1-III expression accelerated several aspects of SMA motor axon development including Schwann cell number, segregation, myelination, and radial growth. These morphological changes have functional consequences accelerating motor axon conduction velocity neonatally.

In the neuromuscular system, NRG1-III is expressed at high levels by MNs during development [17, 32] and is localized to the surface of their axons regulating the differentiation and survival of Schwann cells. A minimal threshold of NRG1-III expression by individual axons

signals the Schwann cell cytoplasm to ensheath it [47]. Subsequent high expression levels by larger axons stimulates segregation into a 1:1 relationship with Schwann cells as well as formation of myelin sheaths [33, 47] that enable saltatory conduction. In contrast, lower levels of NRG1-III expression by autonomic or small sensory axons leads to ensheathment of multiple unmyelinated axons by a single Schwann cell together in a Remak bundle [47]. We have previously shown in severe human SMA mouse VRs at the time of autopsy and in L1 VRs at embryonic and early postnatal time points in SMA $\Delta$ 7 mice that there is an excess of axons with immature morphologies including the most immature abutting axons within single Schwann cell pockets, and reduced acquisition of myelinated axons [22]. Given this phenotype, it is not surprising to observe reduced NRG1 expression in a proportion of SMA axons. The reduction of NRG1-III mRNA levels in the spinal cord is consistent with this arising at least in part from reduced transcription and/or impaired mRNA processing. This could be directly caused by SMN protein deficiency as SMA is required for maintaining the fidelity of spliceosome small nuclear ribonucleoproteins (snRNPs) and NRG1 transcripts undergo

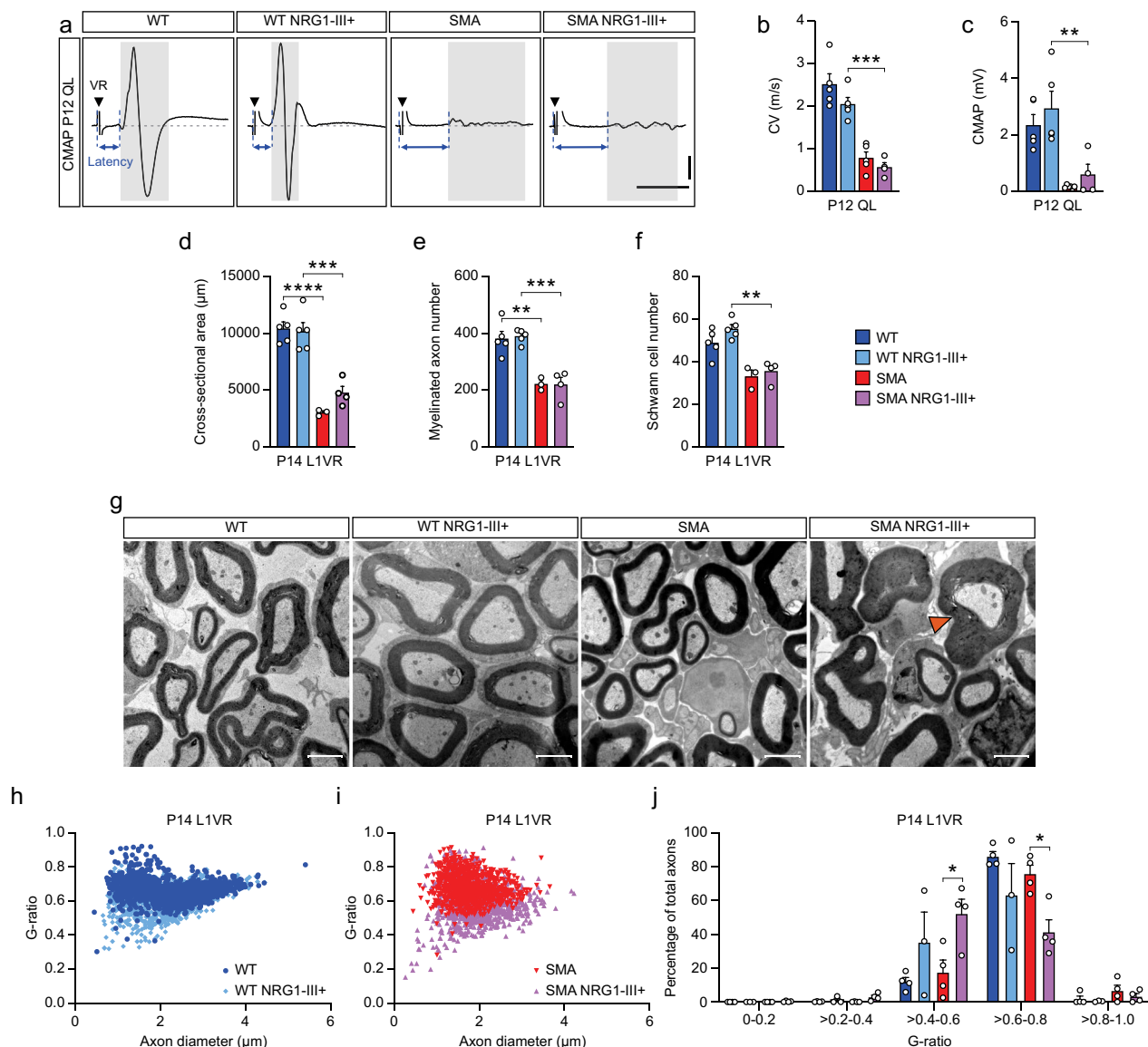


**Fig. 5** NRG1-III overexpression does not provide sustained improvement to SMA motor axon morphology or function **A** Representative EMG traces from the QL muscle in P12 mice. **B** Conduction velocity from the QL muscle of WT (n = 5), WT NRG1-III + (n = 5), SMA (n = 5), and SMA NRG1-III + (n = 4) mice at P12. **C** CMAP amplitude from the QL muscle of WT (n = 5), WT NRG1-III + (n = 5), SMA (n = 6), and SMA NRG1-III + (n = 4) mice at P12. **D** Cross-sectional area, **E** myelinated axon number and **F** Schwann cell number of L1 VRs in WT (n = 5), WT NRG1-III + (n = 5), SMA (n = 3), and SMA NRG1-III + (n = 4) mice at P14. **G** Representative EM images of L1 VRs in WT, WT NRG1-III +, SMA, and SMA NRG1-III + mice at P14 (scale bar: 2 µm). The orange arrow indicates a large myelin sheath. **(H and I)** Axon diameters and G-ratios of L1 VRs in WT and WT NRG1-III + **H** and SMA and SMA NRG1-III + **I** P14 mice. **J** Percentage of axons by axon diameter in L1 VR of WT (n = 4), WT NRG1-III + (n = 3), SMA (n = 4), and SMA NRG1-III + (n = 4) mice at P14. Data represents means and SEM. Statistical analysis was performed in **(B)–(F)** using one-way ANOVA; and in **(J)** using unpaired t test. Significance of WT compared to SMA NRG1-III + and WT NRG1-III + compared to SMA not included. Significance: \* $p \leq .05$ , \*\* $p < 0.01$ , \*\*\* $p < 0.001$ , \*\*\*\* $p < 0.0001$

extensive alternative splicing [7]. Alternatively, reduced NRG1-III expression may be triggered as a downstream cellular consequence of SMN deficiency such as impaired SMA MN firing [14, 30]. NRG1 type I and IV expression have been shown to be activated by neuronal activity in primary cortical neurons [27]. Consistent with the

conclusion that NRG1-III deficiency directly contributes to poor neonatal axon development in SMA, boosting NRG1-III expression accelerated L1 VR axon-Schwann cell developmental interactions including axon segregation and myelination with associated increased VR size, Schwann cell and myelinated axon number. Interestingly,

these improvements in myelination were also associated with an increase in axon diameter in SMA NRG1-III mice, which might be secondary to the influence of increased myelination on the trafficking and post-translational modifications of NFs, whose assembly determines axonal radial diameter [10, 18, 37]. Together these pathological changes increased axon conduction velocity at P2. Unfortunately, despite the critical role for Schwann cells in providing neurotrophic and metabolic support to axons [4, 38], the developmental improvements in the relationships between SMA Schwann cells and motor axons were not sufficient to prevent distal axon degeneration at SMA NMJs and consequently, there was no improvement in the CMAP amplitudes.

In addition to its localization to axons, NRG1 is also present at cholinergic synapses including the postsynaptic terminal of C-terminal boutons on MN somata and at NMJs. A previously published study reported a transient increase in NRG1 positive C terminal boutons at P1 in SMA $\Delta$ 7 compared to WT mice and equivalent numbers at P7 and P15 [15], however the specific lumbar spinal level examined was not defined in this study. Here, we observed a late loss of NRG1 + MN punctae on L1 and L5 medial column MNs, but not L5 lateral column MNs corresponding to those distributions known to be susceptible to axonal degeneration in this model [22]. Loss of NRG1 + punctae intensity on MNs has also been previously observed in the setting of axotomy and in ALS mice [15, 43]. C-terminal boutons are postulated to play an important role in driving MN activity [34, 50]. Whether this is an important contributor to the altered MN firing that has been described in SMA mice [6, 14] will require further study. At the NMJ, NRG1-III signaling is not required for NMJ formation [11, 19], but it has been reported to regulate the behavior of terminal Schwann cells. Neonatal transgenic mice overexpressing NRG1-III have been shown to have an increased number of terminal Schwann cells and accelerated removal of polyneuronal innervation at the NMJ perhaps via enhanced phagocytic activity of these cells [23]. Of note, SMA mice have been reported to have a reduced number of terminal Schwann cells together with a reduced rate of polyneuronal innervation removal [24]. NRG1-III overexpression in the SMA background may have accelerated NMJ pruning events mitigating the positive developmental effects seen at more proximal motor axons.

This work provides a proof-of-principle that SMA motor axon developmental pathologies can be mitigated by molecular strategies independent of increasing SMN expression. NRG1-III has been explored as a therapeutic strategy in preclinical models of genetic neuropathy [2] and in ALS, [35, 36] the later using adeno-associated

virus vectors expressing NRG1-III. Although a potential therapeutic strategy in several diseases, successful translation of NRG1-III to humans will require advances in targeted delivery strategies to prevent untoward effects as NRG1 is also widely expressed in the brain. Older Thy1.2-HA-NRG1-III mice develop cortical synaptic dysfunction with associated anxiety-like behaviors [1]. Such untoward effects may have contributed to the poor behavioral and survival outcomes of older SMA mice transgenically overexpressing NRG1-III seen here. Further work is needed to identify methods to deliver NRG1-III specifically to MNs and to assess outcomes in SMA mouse models when NRG1-III is delivered together with current SMN induction therapies. While our study indicates that NRG1-III is one molecular determinant of axon maldevelopment in SMA, further characterization of the molecular mechanisms underlying impaired development and degeneration of SMA motor axons is urgently needed. Our previous work indicates that these events are largely MN cell autonomous as accelerated motor axon development was seen in mice with increased SMN expression in MNs, but not in mice with increased SMN expression in Schwann cells or muscle [22]. Peripheral axon development depends on multiple molecular mediators expressed specifically by Schwann cells or by axons such as adhesion molecules, components of the extracellular matrix, Notch signaling components and Nectin proteins [12, 46]. Most of the mediators identified to date are expressed by Schwann cells with those expressed by axons remaining largely unknown. Continued unbiased molecular phenotyping of developing WT and SMA motor axons is required to identify such neuronally expressed factors.

Strategies to accelerate SMA motor axon development and prevent degeneration promise to be complementary to existing disease modifying therapeutics, which increase SMN expression, but vary in their therapeutic efficacy. Here we identify NRG1-III as a key molecular determinant of impaired motor axon segregation and myelination in SMA. Furthermore, we demonstrate that boosting NRG1-III expression accelerates several steps of SMA neonatal motor axon maturation. This work illustrates the potential of targeting developmental pathways downstream of SMN protein deficiency as a means to ameliorate aspects of disease pathology that cannot be reversed by postnatal SMN protein induction alone.

### Supplementary Information

The online version contains supplementary material available at <https://doi.org/10.1186/s40478-023-01551-8>.

**Additional file 1: Fig. S1.** SMN protein expression in WT and SMA mice overexpressing NRG1-III. A SMN protein expression in representative western blots of spinal cord tissues collected from WT (n = 3), WT NRG1-III+ (n

= 3), SMA (n = 3), and SMA NRG1-III+ (n = 2) mice at P10. B Quantification of relative SMN expression in western blot in (A).

**Additional file 2: Fig. S2.** NRG1-III overexpression fails to improve motor behavior and survival of SMA mice (A–C) Survival, A weight, B and righting time C of WT (n = 9), WT NRG1-III+ (n = 15), SMA (n = 18), and SMA NRG1-III+ (n = 12) mice. Data represents means and SEM. Statistical analysis was performed using log-rank test in (A). Significance: \*\*\**p* < 0.001.

#### Acknowledgements

We would like to express our gratitude for the generosity and altruism of donors and their families, whose gifts of tissues serve an integral role in advancing medical research and education. Some human tissues were received from the NIH NeuroBioBank at the University of Maryland (Baltimore, MD). We thank Nadav Weinstock with help with EM imaging. We thank Lawrence Wrabetz for providing Thy1.2-HA-NRG1-III mice from the University of Buffalo.

#### Author contributions

LK, CWH, FG, JMB, JBP, MHS, CMS, and CJS designed the research studies. LK, CWH, FG, JMB, JBP, DOV, MHCC, JR, MHS, CMS and CJS conducted experiments. LK, CWH, FG, JMB, JBP, DOV, AM, AC, JR, SAM, MD, SB, CMS, and CJS acquired data. LK, CWH, FG, JMB, JBP, DOV, AM, AC, SAM, MD, SB, CMS, and CJS analyzed data. LK, CWH, FG, JMB, CMS, and CJS wrote the manuscript. LK, CWH, FG, JMB, MHS, CMS, and CJS critically revised the manuscript. All authors read and approved the final manuscript.

#### Funding

This work was supported by funding NIH (R35 NS122306) to CJS, from NIH (R25 GM109441) to CH, and the German Research Foundation grants SI-1969/2-1, SI-1969/3-1, and SMA Europe to CMS.

#### Availability of data and materials

All data generated and/or analyzed during this study are included in this published article.

#### Declarations

##### Ethics approval and consent to participate

Human autopsy tissues were collected following parental- or patient-informed consent in strict observance of legal and institutional ethical regulations. Protocols were approved by the Institutional Review Boards at the Johns Hopkins University School of Medicine. Mouse studies were performed in accordance with the National Institutes of Health Guide for Care and Use of Laboratory Animals, and approved by Institutional Animal Care and Use Committees (IACUCs) at Johns Hopkins University School of Medicine and Leipzig University.

##### Consent for publication

Not applicable.

##### Competing interests

The authors declare that they have no competing interests.

##### Author details

<sup>1</sup>Departments of Neurology, Johns Hopkins University School of Medicine, 855 North Wolfe Street, Rangos Building Room 234, Baltimore, MD 21205, USA. <sup>2</sup>Carl-Ludwig-Institute for Physiology, Leipzig University, Leipzig, Germany. <sup>3</sup>Department of Neuropathology, University Hospital Leipzig, Leipzig, Germany. <sup>4</sup>Departments of Neuroscience, Johns Hopkins University School of Medicine, Baltimore, MD 21205, USA.

Received: 2 February 2023 Accepted: 12 March 2023

Published online: 30 March 2023

#### References

- Agarwal A, Zhang M, Trembak-Duff I, Unterbarnscheidt T, Radyushkin K, Dibaj P, Martins de Souza D, Boretius S, Brzozka MM, Steffens H et al (2014) Dysregulated expression of neuregulin-1 by cortical pyramidal neurons disrupts synaptic plasticity. *Cell Rep* 8:1130–1145. <https://doi.org/10.1016/j.celrep.2014.07.026>
- Belin S, Ornaghi F, Shackelford G, Wang J, Scapin C, Lopez-Anido C, Silvestri N, Robertson N, Williamson C, Ishii A et al (2019) Neuregulin 1 type III improves peripheral nerve myelination in a mouse model of congenital hypomyelinating neuropathy. *Hum Mol Genet* 28:1260–1273. <https://doi.org/10.1093/hmg/ddy420>
- Birchmeier C, Bennett DL (2016) Neuregulin/ErbB signaling in developmental myelin formation and nerve repair. *Curr Top Dev Biol* 116:45–64. <https://doi.org/10.1016/bs.ctdb.2015.11.009>
- Bosch-Queralt M, Fledrich R, Stassart RM (2023) Schwann cell functions in peripheral nerve development and repair. *Neurobiol Dis* 176:105952. <https://doi.org/10.1016/j.nbd.2022.105952>
- Buettner JM, Kirmann T, Mentis GZ, Hallermann S, Simon CM (2022) Laser microscopy acquisition and analysis of premotor synapses in the murine spinal cord. *STAR Protoc* 3:101236. <https://doi.org/10.1016/j.xpro.2022.101236>
- Buettner JM, Sime Longang JK, Gerstner F, Apel KS, Blanco-Redondo B, Sowoidnich L, Janzen E, Langenhan T, Wirth B, Simon CM (2021) Central synaptopathy is the most conserved feature of motor circuit pathology across spinal muscular atrophy mouse models. *iScience* 24:103376. <https://doi.org/10.1016/j.isci.2021.103376>
- Buonanno A (2010) The neuregulin signaling pathway and schizophrenia: from genes to synapses and neural circuits. *Brain Res Bull* 83:122–131. <https://doi.org/10.1016/j.brainresbull.2010.07.012>
- Darras BT, Crawford TO, Finkel RS, Mercuri E, De Vivo DC, Oskoui M, Tizzano EF, Ryan MM, Muntoni F, Zhao G et al (2019) Neurofilament as a potential biomarker for spinal muscular atrophy. *Ann Clin Transl Neurol* 6:932–944. <https://doi.org/10.1002/acn3.779>
- De Vivo DC, Bertini E, Swoboda KJ, Hwu WL, Crawford TO, Finkel RS, Kirschner J, Kuntz NL, Parsons JA, Ryan MM et al (2019) Nusinersen initiated in infants during the presymptomatic stage of spinal muscular atrophy: Interim efficacy and safety results from the phase 2 NURTURE study. *Neuromuscul Disord* 29:842–856. <https://doi.org/10.1016/j.nmd.2019.09.007>
- de Waegh SM, Lee VM, Brady ST (1992) Local modulation of neurofilament phosphorylation, axonal caliber, and slow axonal transport by myelinating Schwann cells. *Cell* 68:451–463. [https://doi.org/10.1016/0092-8674\(92\)90183-d](https://doi.org/10.1016/0092-8674(92)90183-d)
- Escher P, Lacazette E, Courtet M, Blindenbacher A, Landmann L, Bezakova G, Lloyd KC, Mueller U, Brenner HR (2005) Synapses form in skeletal muscles lacking neuregulin receptors. *Science* 308:1920–1923. <https://doi.org/10.1126/science.1108258>
- Feltri ML, Poitelon Y, Previtali SC (2016) How Schwann cells sort axons: new concepts. *Neuroscientist* 22:252–265. <https://doi.org/10.1177/1073858415572361>
- Fledrich R, Kungl T, Nave KA, Stassart RM (2019) Axioglia interdependence in peripheral nerve development. *Development* 146:151704. <https://doi.org/10.1242/dev.151704>
- Fletcher EV, Simon CM, Pagiazitis JG, Chalif JI, Vukojicic A, Drobac E, Wang X, Mentis GZ (2017) Reduced sensory synaptic excitation impairs motor neuron function via Kv2.1 in spinal muscular atrophy. *Nat Neurosci* 20:905–916. <https://doi.org/10.1038/nn.4561>
- Gallart-Palau X, Tarabal O, Casanovas A, Sabado J, Correa FJ, Hereu M, Piedrafita L, Caldero J, Esquerda JE (2014) Neuregulin-1 is concentrated in the postsynaptic subsurface cistern of C-bouton inputs to alpha-motoneurons and altered during motoneuron diseases. *FASEB J* 28:3618–3632. <https://doi.org/10.1096/fj.13-248583>
- Hashimoto R, Straub RE, Weickert CS, Hyde TM, Kleinman JE, Weinberger DR (2004) Expression analysis of neuregulin-1 in the dorsolateral prefrontal cortex in schizophrenia. *Mol Psychiatry* 9:299–307. <https://doi.org/10.1038/sj.mp.4001434>

17. Ho WH, Armanini MP, Nuijens A, Phillips HS, Osheroff PL (1995) Sensory and motor neuron-derived factor. A novel heregulin variant highly expressed in sensory and motor neurons. *J Biol Chem* 270:26722
18. Hsieh ST, Kidd GJ, Crawford TO, Xu Z, Lin WM, Trapp BD, Cleveland DW, Griffin JW (1994) Regional modulation of neurofilament organization by myelination in normal axons. *J Neurosci* 14:6392–6401. <https://doi.org/10.1523/JNEUROSCI.14-11-06392.1994>
19. Jaworski A, Burden SJ (2006) Neuromuscular synapse formation in mice lacking motor neuron- and skeletal muscle-derived Neuregulin-1. *J Neurosci* 26:655–661. <https://doi.org/10.1523/JNEUROSCI.4506-05.2006>
20. Kariyawasam D, D'Silva A, Howells J, Herbert K, Geelan-Small P, Lin CS, Farrar MA (2020) Motor unit changes in children with symptomatic spinal muscular atrophy treated with nusinersen. *J Neurol Neurosurg Psychiatry* 92:78–85. <https://doi.org/10.1136/jnnp-2020-324254>
21. Kariyawasam DST, D'Silva AM, Herbert K, Howells J, Carey K, Kandula T, Farrar MA, Lin CS (2022) Axonal excitability changes in children with spinal muscular atrophy treated with nusinersen. *J Physiol* 600:95–109. <https://doi.org/10.1113/JP282249>
22. Kong L, Valdivia DO, Simon CM, Hassinan CW, Delestree N, Ramos DM, Park JH, Pilato CM, Xu X, Crowder M et al (2021) Impaired prenatal motor axon development necessitates early therapeutic intervention in severe SMA. *Sci Transl Med* 13:eabb6871. <https://doi.org/10.1126/scitranslmed.abb6871>
23. Lee YI, Li Y, Mikesch M, Smith I, Nave KA, Schwab MH, Thompson WJ (2016) Neuregulin1 displayed on motor axons regulates terminal Schwann cell-mediated synapse elimination at developing neuromuscular junctions. *Proc Natl Acad Sci U S A* 113:E479–487. <https://doi.org/10.1073/pnas.1519156113>
24. Lee YI, Mikesch M, Smith I, Rimer M, Thompson W (2011) Muscles in a mouse model of spinal muscular atrophy show profound defects in neuromuscular development even in the absence of failure in neuromuscular transmission or loss of motor neurons. *Dev Biol* 356:432–444. <https://doi.org/10.1016/j.ydbio.2011.05.667>
25. Lefebvre S, Burglen L, Reboullet S, Clermont O, Bulet P, Viollet L, Benichou B, Cruaud C, Millasseau P, Zeviani M et al (1995) Identification and characterization of a spinal muscular atrophy-determining gene. *Cell* 80:155–165. [https://doi.org/10.1016/0092-8674\(95\)90460-3](https://doi.org/10.1016/0092-8674(95)90460-3)
26. Lefebvre S, Bulet P, Liu Q, Bertrand S, Clermont O, Munnich A, Dreyfuss G, Melki J (1997) Correlation between severity and SMN protein level in spinal muscular atrophy. *Nat Genet* 16:265–269. <https://doi.org/10.1038/ng0797-265>
27. Liu X, Bates R, Yin DM, Shen C, Wang F, Su N, Kirov SA, Luo Y, Wang JZ, Xiong WC et al (2011) Specific regulation of NRG1 isoform expression by neuronal activity. *J Neurosci* 31:8491–8501. <https://doi.org/10.1523/JNEUROSCI.5317-10.2011>
28. Lorson CL, Hahnen E, Androphy EJ, Wirth B (1999) A single nucleotide in the SMN gene regulates splicing and is responsible for spinal muscular atrophy. *Proc Natl Acad Sci U S A* 96:6307–6311. <https://doi.org/10.1073/pnas.96.11.6307>
29. Martinez TL, Kong L, Wang X, Osborne MA, Crowder ME, Van Meerbeke JP, Xu X, Davis C, Wooley J, Goldhamer DJ et al (2012) Survival motor neuron protein in motor neurons determines synaptic integrity in spinal muscular atrophy. *J Neurosci* 32:8703–8715. <https://doi.org/10.1523/JNEUROSCI.0204-12.2012>
30. Mentis GZ, Liu W, Blivis D, Drobac E, Crowder ME, Kong L, Alvarez FJ, Sumner CJ, O'Donovan MJ (2011) Early functional impairment of sensory-motor connectivity in a mouse model of spinal muscular atrophy. *Neuron* 10:453–467. <https://doi.org/10.1016/j.neuron.2010.12.032>
31. Mercuri E, Sumner CJ, Muntoni F, Darras BT, Finkel RS (2022) Spinal muscular atrophy. *Nat Rev Dis Primers* 8:52. <https://doi.org/10.1038/s41572-022-00380-8>
32. Meyer D, Yamaai T, Garratt A, Riethmacher-Sonnenberg E, Kane D, Theill LE, Birchmeier C (1997) Isoform-specific expression and function of neuregulin. *Development* 124:3575–3586. <https://doi.org/10.1242/dev.124.18.3575>
33. Michailov GV, Sereda MW, Brinkmann BG, Fischer TM, Haug B, Birchmeier C, Role L, Lai C, Schwab MH, Nave KA (2004) Axonal neuregulin-1 regulates myelin sheath thickness. *Science* 304:700–703. <https://doi.org/10.1126/science.1095862>
34. Miles GB, Hartley R, Todd AJ, Brownstone RM (2007) Spinal cholinergic interneurons regulate the excitability of motoneurons during locomotion. *Proc Natl Acad Sci U S A* 104:2448–2453. <https://doi.org/10.1073/pnas.0611134104>
35. Modol-Caballero G, Garcia-Lareu B, Verdes S, Ariza L, Sanchez-Brualla I, Brocard F, Bosch A, Navarro X, Herrando-Grabulosa M (2020) Therapeutic role of neuregulin 1 type III in SOD1-linked amyotrophic lateral sclerosis. *Neurotherapeutics* 17:1048–1060. <https://doi.org/10.1007/s13311-019-00811-7>
36. Modol-Caballero G, Herrando-Grabulosa M, Verdes S, Garcia-Lareu B, Hernandez N, Francos-Quijorna I, Lopez-Vales R, Bosch A, Navarro X (2021) Gene therapy overexpressing neuregulin 1 type I in combination with neuregulin 1 type III promotes functional improvement in the SOD1(G93A) ALS mice. *Front Neurol* 12:693309. <https://doi.org/10.3389/fneur.2021.693309>
37. Monsma PC, Li Y, Fenn JD, Jung P, Brown A (2014) Local regulation of neurofilament transport by myelinating cells. *J Neurosci* 34:2979–2988. <https://doi.org/10.1523/JNEUROSCI.4502-13.2014>
38. Nave KA (2010) Myelination and the trophic support of long axons. *Nat Rev Neurosci* 11:275–283. <https://doi.org/10.1038/nrn2797>
39. Nave KA, Salzer JL (2006) Axonal regulation of myelination by neuregulin 1. *Curr Opin Neurobiol* 16:492–500. <https://doi.org/10.1016/j.conb.2006.08.008>
40. Ou GY, Lin WW, Zhao WJ (2021) Neuregulins in neurodegenerative diseases. *Front Aging Neurosci* 13:662474. <https://doi.org/10.3389/fnagi.2021.662474>
41. Pilato CM, Park JH, Kong L, d'Ydewalle C, Valdivia D, Chen KS, Griswold-Prenner I, Sumner CJ (2019) Motor neuron loss in SMA is not associated with somal stress-activated JNK/c-Jun signaling. *Hum Mol Genet* 28:3282–3292. <https://doi.org/10.1093/hmg/ddz150>
42. Ramos DM, d'Ydewalle C, Gabbeta V, Dakka A, Klein SK, Norris DA, Matson J, Taylor SJ, Zaworski PG, Prior TW et al (2019) Age-dependent SMN expression in disease-relevant tissue and implications for SMA treatment. *J Clin Invest* 129:4817–4831. <https://doi.org/10.1172/JCI124120>
43. Salvany S, Casanovas A, Tarabal O, Piedrafita L, Hernandez S, Santafe M, Soto-Bernardini MC, Caldero J, Schwab MH, Esquerda JE (2019) Localization and dynamic changes of neuregulin-1 at C-type synaptic boutons in association with motor neuron injury and repair. *FASEB J* 33:7833–7851. <https://doi.org/10.1096/fj.201802329R>
44. Shi L, Bergson CM (2020) Neuregulin 1: an intriguing therapeutic target for neurodevelopmental disorders. *Transl Psychiatry* 10:190. <https://doi.org/10.1038/s41398-020-00868-5>
45. Stassart RM, Fledrich R, Velanac V, Brinkmann BG, Schwab MH, Meijer D, Sereda MW, Nave KA (2013) A role for Schwann cell-derived neuregulin-1 in remyelination. *Nat Neurosci* 16:48–54. <https://doi.org/10.1038/nn.3281>
46. Taveggia C (2016) Schwann cells-axon interaction in myelination. *Curr Opin Neurobiol* 39:24–29. <https://doi.org/10.1016/j.conb.2016.03.006>
47. Taveggia C, Zanazzi G, Petrylak A, Yano H, Rosenbluth J, Einheber S, Xu X, Esper RM, Loeb JA, Shrager P et al (2005) Neuregulin-1 type III determines the ensheathment fate of axons. *Neuron* 47:681–694. <https://doi.org/10.1016/j.neuron.2005.08.017>
48. Velanac V, Unterbarnscheidt T, Hinrichs W, Gummert MN, Fischer TM, Rossner MJ, Trimarco A, Brivio V, Taveggia C, Willem M et al (2012) Bace1 processing of NRG1 type III produces a myelin-inducing signal but is not essential for the stimulation of myelination. *Glia* 60:203–217. <https://doi.org/10.1002/glia.21255>
49. Webster HD, Martin R, O'Connell MF (1973) The relationships between interphase Schwann cells and axons before myelination: a quantitative electron microscopic study. *Dev Biol* 32:401–416. [https://doi.org/10.1016/0012-1606\(73\)90250-9](https://doi.org/10.1016/0012-1606(73)90250-9)
50. Zagoraoui L, Akay T, Martin JF, Brownstone RM, Jessell TM, Miles GB (2009) A cluster of cholinergic premotor interneurons modulates mouse locomotor activity. *Neuron* 64:645–662. <https://doi.org/10.1016/j.neuron.2009.10.017>

## Publisher's Note

Springer Nature remains neutral with regard to jurisdictional claims in published maps and institutional affiliations.